



Published in final edited form as:

Nat Med. 2009 January ; 15(1): 50–58. doi:10.1038/nm.1900.

## Gamma-secretase inhibitors reverse glucocorticoid resistance in T-ALL

Pedro J. Real<sup>1,2</sup>, Valeria Tosello<sup>1,11</sup>, Teresa Palomero<sup>1,3,11</sup>, Mireia Castillo<sup>3</sup>, Eva Hernando<sup>4</sup>, Elisa de Stanchina<sup>5</sup>, Maria Luisa Sulis<sup>1,6</sup>, Kelly Barnes<sup>1</sup>, Catherine Sawai<sup>7</sup>, Irene Homminga<sup>8</sup>, Jules Meijerink<sup>8</sup>, Iannis Aifantis<sup>7</sup>, Giuseppe Basso<sup>9</sup>, Carlos Cordon-Cardo<sup>3</sup>, Walden Ai<sup>10</sup>, and Adolfo Ferrando<sup>1,3,6</sup>

<sup>1</sup>Institute for Cancer Genetics-Columbia University, New York, NY, 10032, USA <sup>2</sup>Andalusian Stem Cell Bank, Centro de Investigacion Biomedica, Granada, 18100, Spain <sup>3</sup>Department of Pathology, Columbia University Medical Center, New York, NY, 10032, USA <sup>4</sup>Department of Pathology, NYU Medical Center, New York, NY, 10016, USA <sup>5</sup>Antitumor assessment Core Facility, Memorial Sloan-Kettering Cancer Center, New York, NY, 10021 <sup>6</sup>Department of Pediatrics, Columbia University Medical Center, New York, NY, 10032, USA <sup>7</sup>Department of Pathology, NYU Cancer Institute, New York, NY, 10016 <sup>8</sup>Department of Pediatric Oncology/Hematology, Erasmus MC-Sophia Children's Hospital, Rotterdam, 3015GJ, The Netherlands <sup>9</sup>Hemato-Oncology Laboratory, Department of Pediatrics, University of Padua, Padua, 35128, Italy <sup>10</sup>Department of Pathology, Microbiology and Immunology, University of South Carolina School of Medicine, Columbia, SC 29208

### Summary

Gamma-secretase inhibitors (GSIs) block the activation of oncogenic NOTCH1 in T-cell acute lymphoblastic leukemia (T-ALL). However, limited antileukemic cytotoxicity and severe gastrointestinal toxicity have restricted the clinical application of these targeted drugs. Here we show that combination therapy with GSIs plus glucocorticoids can improve the antileukemic effects of GSIs and reduce their gut toxicity *in vivo*. Inhibition of NOTCH1 signaling in glucocorticoid-resistant T-ALL restored glucocorticoid receptor auto-up-regulation and induced apoptotic cell death through induction of *BIM* expression. GSI treatment resulted in cell cycle arrest and accumulation of goblet cells in the gut mediated by upregulation of *Klf4*, a negative regulator of cell cycle required for goblet cell differentiation. In contrast, glucocorticoid treatment induced transcriptional upregulation of *Ccnd2* and protected mice from developing intestinal

Users may view, print, copy, and download text and data-mine the content in such documents, for the purposes of academic research, subject always to the full Conditions of use:[http://www.nature.com/authors/editorial\\_policies/license.html#terms](http://www.nature.com/authors/editorial_policies/license.html#terms)

<sup>11</sup>Valeria Tosello and Teresa Palomero contributed equally to this work

#### Author contributions

A.F. supervised the project. P.R., V.T., T.P., M.L.S., K.B., C.S. and I.H. performed experiments. M.C. performed histological and immunohistochemical studies. E.H. and E.S. assisted in bioimaging analysis of tumor xenografts. G.B. provided clinical samples. J.M. provided clinical samples and supervised drug sensitivity assays in these cells. A.F. and I.A. supervised the analysis of *Ccnd2*<sup>-/-</sup> mice. C.C.C. supervised histological and immunohistochemical studies. A.F. wrote the manuscript.

**Microarray data repository information.** Microarray data is available at GEO (accession numbers GSE7067 and GSE11184).

#### Competing interests statement

The authors declare that they have no competing financial interest

goblet cell metaplasia typically induced by inhibition of NOTCH signaling with GSIs. These results support a role for glucocorticoids plus GSIs in the treatment of glucocorticoid-resistant T-ALL.

## Introduction

Gamma-secretase inhibitors (GSIs), which block the presenilin-gamma secretase complex, inhibit the production of amyloidogenic A $\beta$  peptides involved in the pathogenesis of Alzheimer's disease and the activation of NOTCH receptors 1,2. Recent identification of activating mutations in the *NOTCH1* receptor gene in over 50% of cases of T-cell lymphoblastic leukemia (T-ALL) 3 prompted the initiation of a clinical trial to test the effectiveness of blocking NOTCH1 signaling with a small molecule GSI in this disease 4,5. However, the clinical development of GSI-based therapies has been hampered by the limited ability of these drugs to induce apoptosis in human T-ALL 6,7 and by the development of severe gastrointestinal toxicity due to inhibition of NOTCH signaling in the gut 5,8–11.

Here, we show that inhibition of NOTCH1 signaling with a GSI can reverse glucocorticoid resistance in T-ALL and that dexamethasone cotreatment protects mice from severe secretory metaplasia 8–11 induced by inhibition of NOTCH signaling in the gut.

## Results

### GSI treatment reverses glucocorticoid resistance in T-ALL

NOTCH1 signaling plays an important role in the specification of cell fate and maintenance of cell tropism during T-cell development 12,13. Aberrant NOTCH1 signaling can protect developing thymocytes against glucocorticoid-induced cell death 14 and is a critical oncogenic event in the pathogenesis of T-ALL 15–17. To test if aberrant NOTCH1 signaling might contribute to glucocorticoid resistance in T-ALL, we analyzed the responses of human T-ALL cells to increased doses of dexamethasone in the presence of CompE, a highly active GSI 18. CUTLL1, a well-characterized T-cell lymphoblastic cell line with activated NOTCH1 6 is highly resistant to glucocorticoids, showing only a minimal loss of cell viability when treated with dexamethasone concentrations as high as  $10^{-5}$  M (Fig. 1a). Treatment of CUTLL1 cells with 100 nM CompE for 72 hours effectively blocks NOTCH1 signaling and induces a modest cytostatic response characterized by G1 cell cycle arrest (Supplementary Fig. 1 online) 6,19,20. By contrast, treatment of CUTLL1 cells with dexamethasone in the presence of CompE (100 nM) effectively impaired cell viability, with an  $IC_{50}$  value of  $7.7 \times 10^{-8}$  M for dexamethasone in the presence of CompE at 72 hours (Fig. 1a). Similarly, dose response analysis of CUTLL1 cells treated with dexamethasone (100 nM) and a range of CompE concentrations showed a synergistic dose dependent response to this GSI in combination with dexamethasone (Supplementary Fig. 2 online). Subsequent analysis of KOPTK1 and TALL1, two additional glucocorticoid-resistant T-ALL cell lines that respond with G1 cell cycle arrest upon CompE treatment (Supplementary Fig. 1 online) 3, showed significant decreases in cell viability when treated with both dexamethasone and CompE, indicative of a synergistic interaction between these agents (Fig. 1a). Analysis of glucocorticoid-sensitive cell lines (DND41 and P12-ICHIKAWA) or

B-cell derived tumors devoid of NOTCH1 activation (Raji and Ramos) showed no evidence of synergistic interaction between CompE and dexamethasone (Fig. 1b). Similarly, analysis of 8 T-ALL primary samples from patients at relapse showed synergistic interaction between CompE and dexamethasone in 2 out of 3 glucocorticoid resistant tumors, but not in leukemias retaining glucocorticoid sensitivity (Fig. 1c and Supplementary Fig. 3 online).

The synergistic effects of CompE plus dexamethasone observed in CUTLL1 cells were reversed by treatment with RU486, a glucocorticoid receptor antagonist (Fig. 1d). Similarly, expression of an intracellular activated NOTCH1 (ICN1), which does not require  $\gamma$ -secretase cleavage, bypassed the inhibitory effects of GSIs in NOTCH1 signaling, and protected CUTLL1 cells from the effects of dexamethasone plus CompE cotreatment (Fig. 1e and Supplementary Fig. 4 online). These data, together with the lack of synergism between CompE and other antileukemic drugs (Supplementary Fig. 5) demonstrates a specific interaction between GSIs and glucocorticoids in T-ALL.

Next we asked if the synergistic effects of CompE plus dexamethasone reflect enhanced apoptotic responses to glucocorticoid therapy. Annexin V-PI staining demonstrated increased apoptosis in CUTLL1, KOPTK1, and TALL1 cells treated with CompE and dexamethasone for 48–72 hours (Fig. 1f). Additionally, Western blot analysis of CUTLL1 cells treated with CompE plus dexamethasone showed a marked increase in PARP cleavage, indicative of activation of effector caspases and apoptosis (Fig. 1g). Furthermore, Z-VAD, a pancaspase inhibitor, reversed the induction of PARP cleavage and apoptosis (detected by annexin V-PI staining) triggered by CompE plus dexamethasone in this cell line (Figs. 1g,h).

### NOTCH1 inhibition restores glucocorticoid receptor autoregulation

Both NOTCH1 and the glucocorticoid receptor function as ligand activated transcription factors, suggesting that crosstalk between NOTCH1 signaling and glucocorticoid therapy may enhance the transcriptional response to dexamethasone in glucocorticoid resistant T-ALL. To analyze the effects of glucocorticoid treatment in the transcriptional regulatory network controlled by NOTCH1 in T-ALL 19 and to explore the mechanisms mediating the reversal of glucocorticoid resistance upon NOTCH inhibition, we performed gene expression profiling with oligonucleotide microarrays in CUTLL1 cells treated with vehicle (DMSO), dexamethasone (1  $\mu$ M), CompE (100 nM) or cotreated with dexamethasone plus CompE for 24 hours. This analysis demonstrated a more efficient glucocorticoid response in cells treated with CompE plus dexamethasone with synergistic upregulation of glucocorticoid regulated genes such as *TSC22D3/GILZ*, *CD53*, *SOCS1* and *BTG2* (Fig. 2a and Supplementary Fig. 6 online). Importantly, the glucocorticoid receptor gene (*NR3C1*) ranked among the top genes synergistically upregulated by dexamethasone plus GSI cotreatment in our microarray analysis (Fig. 2a). Numerous studies on the mechanisms of glucocorticoid resistance have established that an effective upregulation of the glucocorticoid receptor gene in response to glucocorticoids is required for the activation of apoptosis in human leukemias 21–26. Quantitative RT-PCR and Western blot analysis showed a moderate increase in glucocorticoid receptor levels in CUTLL1 cells and primary T-ALL lymphoblasts treated with GSI and dexamethasone (Fig. 2b and Supplementary Figure 3 online). In contrast, dexamethasone plus CompE cotreatment resulted in a

significantly higher (5 fold) upregulation of glucocorticoid receptor transcripts and protein levels (Fig. 2b). These results suggest that inhibition of NOTCH1 signaling enhance glucocorticoid receptor auto-up-regulation and glucocorticoid sensitivity in otherwise glucocorticoid resistant T-ALL cells. Consistent with this hypothesis, and in agreement with previous reports in T-ALL 27–29, retroviral expression of the glucocorticoid receptor gene restored glucocorticoid sensitivity and enhanced the apoptotic response of CUTLL1 cells to dexamethasone (Fig. 2c). Conversely, shRNA knockdown of the glucocorticoid receptor resulted in complete abrogation of apoptosis induced by dexamethasone plus CompE (Fig. 2d)

Glucocorticoid receptor auto-up-regulation has been linked to the function of *NR3C1* promoter *1A* (hematopoietic) and *NR3C1* promoters *1B* and *1C* (ubiquitous) 25,30–32. ChIP-on-chip analysis of HES1, a transcriptional repressor directly controlled by NOTCH1, identified HES1 binding in glucocorticoid receptor promoters 1B and 1C in T-ALL cells (Supplementary Fig. 7 online). Subsequent quantitative ChIP assays confirmed HES1 binding to glucocorticoid receptor promoters 1B and 1C and also demonstrated HES1 binding to regulatory sequences in promoter 1A, which was not represented on the ChIP-on-chip promoter microarray (Fig. 2e). Upregulation of the hematopoietic *NR3C1 A1* promoter is mediated by a 35 base pair regulatory sequence (*FP11-FP12*) which is activated by a NR3C1-MYB heterodimer complex upon glucocorticoid treatment 31. Luciferase reporter assays showed that dexamethasone treatment and MYB expression activated a *NR3C1 A1 FP11-FP12* reporter construct (Fig. 2f). Importantly, *HES1* expression antagonized the activation of the *NR3C1 A1* promoter by dexamethasone, MYB and the combination of glucocorticoid treatment and MYB expression (Fig. 2f). Consistent with these results, HES1 shRNA knockdown in CUTLL1 cells resulted in increased glucocorticoid receptor transcript and protein levels (Fig. 2g) and effective reversal of glucocorticoid resistance (Fig. 2h).

### ***BIM* upregulation reverses glucocorticoid resistance**

Analysis of the expression levels of proapoptotic and antiapoptotic regulators of the mitochondrial cell-death pathway showed that *BIM*, a BH3 only gene required for glucocorticoid-induced apoptosis 33–35, was slightly upregulated by dexamethasone but markedly and synergistically upregulated in CUTLL1 cells treated with dexamethasone plus CompE (Fig. 3a). Similarly, analysis of *BMF*, a BH3-only gene involved in anoikis and cytoskeleton stress-induced apoptosis 36, showed synergistic transcriptional upregulation in cells treated with CompE plus dexamethasone (Fig. 3b). Similar results were obtained in KOPTK1 and TALL1 cells (Supplementary Fig. 8 online). Western blot analysis demonstrated a marked (5 fold) upregulation of proapoptotic BIM isoforms (BIML and BIMS) in CUTLL1 cells treated with CompE plus dexamethasone (Fig. 3c). In contrast, transcriptional upregulation of *BMF* translated into less consistent increases in BMF protein (Fig. 3c). Consistent with these results, shRNA knockdown of *BIM* effectively blocked apoptosis induction by CompE plus dexamethasone cotreatment in CUTLL1 cells (Fig. 3d,e), but downregulation of *BMF* by shRNA knockdown failed to protect these cells from apoptosis induced by such cotreatment (Fig. 3f,g). Together, these results demonstrate that *BIM* upregulation mediates the reversal of glucocorticoid resistance in T-ALL cells treated with dexamethasone plus CompE (Fig. 3h).

### Antileukemic effects of GSI and glucocorticoids *in vivo*

To test whether the synergistic effects of GSI and glucocorticoid cotreatment *in vitro* would enhance the therapeutic efficacy of these agents *in vivo*, we analyzed the effects of dexamethasone and NOTCH inhibition in a xenograft model of glucocorticoid-resistant T-ALL. In these experiments we used DBZ, a highly active GSI, analogous to CompE *in vitro* (Supplementary Fig. 9 online) and with well established activity *in vivo* 8. CUTLL1 cells infected with lentiviruses expressing the luciferase gene were injected subcutaneously in the flanks of immunodeficient (NOD/SCID) mice. After 1 week, animals harboring homogeneous subcutaneous tumors were treated with vehicle only (DMSO), DBZ, dexamethasone or DBZ plus dexamethasone and monitored for 4 days with a bioimaging system to quantify luciferase activity. In this experiment, animals treated with dexamethasone showed progressive tumor growth similar to that observed in vehicle-treated controls, while mice treated with DBZ showed a moderate delay in tumor growth (Fig. 4a,b) consistent with the cytostatic effect of NOTCH1 inhibition with GSIs observed in CUTLL1 cells *in vitro* (Supplementary Fig. 1 online) 6. By contrast, animals treated with DBZ plus dexamethasone had marked antitumor responses with significant reduction in tumor burden after 4 days of treatment (Fig. 4a,b;  $P < 0.01$ ). Importantly, tumor xenografts of CUTLL1 cells expressing the activated intracellular form of NOTCH1 (CUTLL1-ICN1) (Supplementary Fig. 4 online) were unresponsive to the combination of DBZ plus dexamethasone (Fig. 4c), indicating that reversal of glucocorticoid resistance *in vivo* by DBZ treatment is mediated by inhibition of NOTCH1 signaling in the leukemic cells.

To test the significance of these results in a xenograft model that may be a more faithful representation of the natural history of T-ALL patients, CUTLL1 cells expressing the luciferase marker were injected intravenously into irradiated NOD/SCID mice. After 3 weeks, groups of animals with homogeneous tumor burdens were treated with vehicle only, dexamethasone, DBZ or DBZ plus dexamethasone for 2 weeks. Disease progression was readily apparent in control and dexamethasone-treated mice, resulting in tumor-related mortality starting 3 weeks after the initiation of the treatment (Fig. 4d). Animals in the GSI-only treatment group showed low levels of leukemia infiltration compared with DMSO and dexamethasone treated mice. Yet, all of them developed weight loss and accelerated mortality on week 3. Finally, all mice treated with DBZ plus dexamethasone were disease free as determined by *in vivo* bioimaging three weeks after the initiation of the treatment. However, 2 of them were euthanized on day 23 because of excessive (>20%) weight loss. Analysis at the end of the observation period (10 weeks) demonstrated significantly improved survival among mice treated with dexamethasone plus DBZ ( $P < 0.05$  vs. controls).

### Dexamethasone abrogates GSI-induced toxicity in the gut

The poor outcome observed in DBZ treated mice, which harbored low levels of leukemia infiltration, suggested that GSI-induced toxicity might have contributed to their accelerated mortality. Moreover, the improved survival observed in mice treated with DBZ plus dexamethasone suggested that glucocorticoid therapy could ameliorate some of the toxic effects associated with GSI treatment. To test this hypothesis, we analyzed the effects of dexamethasone, DBZ or dexamethasone plus DBZ in of C57/Bl6 mice compared to vehicle-

only treatment controls (Supplementary Fig.10 online). Histological analysis of multiple organs revealed marked changes induced by DBZ treatment in the intestine, thymus and the spleen. Thus, DBZ-treated animals showed severe intestinal secretory metaplasia characterized by a marked increase in the number of goblet cells and arrested cell proliferation (determined by Ki67 immunostaining) in the crypts of the small intestine (Fig. 4e and Supplementary Fig. 11 online). Dexamethasone treatment induced mild changes in the architecture of the gut which were most apparent after 10 days of treatment with moderate elongation of the intestinal crypts and accumulation of Paneth cells at the bottom of the crypt (Fig. 4e, Fig. 6d and Supplementary Fig. 11 online). Importantly, mice cotreated with DBZ plus dexamethasone showed normal goblet cell numbers with preservation of the architecture and proliferation of the intestinal epithelium (Fig. 4e and Supplementary Fig. 11 online).

Importantly, pharmacokinetic analysis ruled out increased DBZ clearance in animals treated with dexamethasone plus DBZ (Supplementary Fig. 12 online) as mechanism of decreased GSI-induced gut toxicity. Moreover, histological analysis of the thymus and spleen showed a synergistic effect of NOTCH inhibition and glucocorticoids in the lymphoid system (Fig. 4e and Supplementary Fig. 13 and Supplementary Fig.14 online).

To analyze if dexamethasone treatment could also ameliorate the effects of NOTCH inactivation via deletion of *CSL/RBPJ*, which encodes the DNA binding protein component of the Notch transcriptional complex 9, we crossed in *RBPJ(f/f)* conditional knockout mice to the *Cre-Tam* mouse line, which expresses a tamoxifen-inducible *Cre* from the ubiquitous *Rosa26* locus 37 and treated the resulting *RBPJ(f/f) Cre-Tam* mice with tamoxifen or tamoxifen plus dexamethasone. In this experiment, animals treated with tamoxifen showed increased numbers of goblet cells induced by ablation of Notch signaling in the gut. In contrast, mice treated with tamoxifen plus dexamethasone were protected from developing goblet cell metaplasia upon genetic inactivation of Notch signaling in the gut (Fig. 4f).

### ***Klf4* upregulation in GSI-induced gut toxicity**

The *Klf4* tumor suppressor gene encodes a Krüppel-like zinc finger transcription factor required for intestinal goblet cell differentiation 38,39. Immunohistochemical analysis of *Klf4* in the intestines of mice treated with DMSO, dexamethasone, DBZ or DBZ plus dexamethasone showed nuclear staining in goblet cells in the villi and in scattered cells in the crypts of control and dexamethasone-treated animals (Fig. 5a). In contrast, animals treated with DBZ showed a marked increase in the number of *Klf4* positive cells in the crypts and in the villi, which was abrogated by glucocorticoid treatment in animals treated with DBZ plus dexamethasone (Fig. 5a,b and Supplementary Fig. 15 online ). Similarly, quantitative RT-PCR analysis showed increased levels of *Klf4* expression in the gut of animals treated with DBZ, but not in animals cotreated with DBZ plus dexamethasone (Fig. 5c), suggesting that Notch signaling could participate in the negative control of *Klf4* expression in the gut. Consistent with this hypothesis, luciferase reporter assays demonstrated that activation of NOTCH signaling by ICN1 downregulates the activity of the *KLF4* promoter in the AGS gastric adenocarcinoma cell line (Fig. 5d) and HCT116 colon adenocarcinoma cells (Supplementary Fig. 16 online). Notably, *Hes1* knockout mice have



increased number of goblet cells in the gut 40 suggesting that Hes1 could work as a transcriptional repressor controlling *Klf4* expression downstream of Notch signaling. Luciferase reporter assays confirmed this hypothesis showing that HES1 expression downregulates the activity of the *KLF4* promoter (Fig. 5d,e). Furthermore, chromatin immunoprecipitation demonstrated binding of HES1 protein to the *KLF4* promoter (Fig. 5f), while shRNA knockdown of HES1 induced upregulation of *KLF4* transcripts (Fig. 5g) and HES1 overexpression downregulated the expression of *KLF4* transcripts (Fig.5h). Overall, these experiments demonstrate that *KLF4* is a direct transcriptional target of HES1 downstream of NOTCH signaling in the gut and support a mechanistic role for *Klf4* upregulation downstream of NOTCH inhibition in GSI-induced gut toxicity.

### ***Ccnd2* upregulation by dexamethasone reverses GSI gut toxicity**

To elucidate the mechanism responsible for the reversal of GSI-induced toxicity in animals treated with glucocorticoids we performed gene expression profiling with oligonucleotide microarrays in the small intestine of mice treated with vehicle (DMSO), dexamethasone, DBZ or the combination of DBZ plus dexamethasone. This analysis identified *Ccnd2*, a critical regulator of cell cycle progression, among the top genes upregulated by dexamethasone (Fig. 6a). Quantitative RT-PCR analysis confirmed that *Ccnd2* expression in the gut was upregulated in animals treated with dexamethasone compared to controls ( $P < 0.001$ ) (Fig. 6b). Importantly, growth arrest and cell differentiation are temporally and functionally linked events in the intestinal epithelium 41, and expression of *Ccnd2* in AGS cells induced a marked decrease in KLF4 transcript levels (Fig. 6c), suggesting that upregulation of *Ccnd2* expression by dexamethasone could mediate at least in part the protective effects of glucocorticoids against GSI-induced goblet cell metaplasia. To address this question, we analyzed the effects of dexamethasone, DBZ or the combination of DBZ plus dexamethasone in *Ccnd2* knockout mice 42. As observed in wild type animals, dexamethasone treatment induced accumulation of Paneth cells at the bottom of the intestinal crypt in *Ccnd2* knockout mice (Fig. 6d,e). However, this increase in cell differentiation towards the Paneth cell lineage was associated with decreased cell numbers and a reduction of Ki67 positive cells per crypt, which was in contrast with the moderate cell expansion induced by glucocorticoid treatment in the intestine of wild type mice (Fig. 6d,e). Moreover, when treated with DBZ plus dexamethasone, *Ccnd2* knockout mice developed GSI-induced goblet cell metaplasia (Fig. 6f), associated with increased levels of KLF4 expression in the gut (Fig. 6g). Importantly, histological analysis of the spleen showed no differences in between wild type and *Ccnd2* deficient animals and served as positive control for the activity of DBZ and dexamethasone in this experiment (Fig. 6f). Overall, these results highlight the functional relevance of *Ccnd2* upregulation induced by dexamethasone treatment for the protection from GSI-induced toxicity in the gut (Fig. 6h).

## **Discussion**

Despite the strong rationale for inhibiting NOTCH1 signaling in the treatment of T-ALL patients harboring activating mutations in the *NOTCH1* gene, progress in clinical testing of GSIs has been hindered by the lack of effective antileukemic cytotoxicity and the development of severe gastrointestinal toxicity 5,8–11,20. Based on the hypothesis that the

combination of NOTCH1 inhibition with chemotherapy could provide an improved therapeutic window, we tested the activity of a GSI with conventional antileukemic agents. These studies showed that inhibition of NOTCH1 signaling can effectively abrogate glucocorticoid resistance in T-ALL primary patient samples and cell lines. Additional pharmacologic interactions affecting glucocorticoid resistance ALL have been described before. Most notably, inhibition of mTOR signaling with rapamycin can reverse glucocorticoid resistance in leukemic lymphoblasts inducing posttranscriptional downregulation of MCL1 43, however we failed to detect changes in the protein levels of this antiapoptotic factor in cells treated with CompE plus dexamethasone (data not shown). Similarly, we did not detect changes in the differentiation arrest of T-ALL cells that could be linked to differential glucocorticoid sensitivity or transcriptional changes in the *SRG3* gene (data not shown), two mechanisms proposed to reduce the sensitivity to glucocorticoid-induced apoptosis downstream of NOTCH1 activation in mouse primary thymocytes 14,44–46.

Analysis of therapeutic efficacy in leukemia-bearing mice cotreated with a highly active GSI plus dexamethasone *in vivo* showed increased antileukemic effects, but also, a surprising decrease in GSI-induced gut toxicity. Molecular analysis of the mechanisms mediating the goblet cell metaplasia induced by inhibition of NOTCH signaling in the gut identified KLF4, a transcription factor responsible for goblet cell differentiation, as a potential mediator of GSI-induced intestinal toxicity. Thus, a possible explanation to account for the protective effects of dexamethasone against GSI-induced gut toxicity *in vivo* would be an inhibitory effect of glucocorticoids in the expression of *Klf4*. However, luciferase reporter assays failed to detect regulation of *KLF4* promoter activity by dexamethasone (Supplementary Fig. 17 online). These negative results suggest that an indirect effect accounts for the downregulation of *KLF4* expression in animals cotreated with a GSI plus dexamethasone.

Detailed characterization of the effects of dexamethasone in the intestinal epithelium showed that glucocorticoids induce a moderate increase in proliferation associated with *Ccnd2* upregulation and promote differentiation of intestinal progenitors into Paneth cells (Fig. 6d). Given that *Klf4* is a negative regulator of cell cycle, we explored the possibility that dexamethasone-induced *Ccnd2* upregulation could antagonize the expression of *Klf4* in the gut. Consistent with this hypothesis, *in vitro* studies in AGS cells showed that forced expression of *Ccnd2* resulted in decreased levels of *KLF4* transcripts (Fig. 6c). Moreover, *in vivo* analysis of *Ccnd2* deficient mice cotreated with a GSI plus dexamethasone showed accumulation of goblet cells and elevated levels of *Klf4* expression, similar to those observed in mice treated with a GSI alone (Fig. 6g). These results suggest that dexamethasone-induced *Ccnd2* upregulation is strictly required for the enteroprotective effects of glucocorticoids against GSI-induced gut toxicity.

Overall, our results support that combination therapies with GSIs plus glucocorticoids may be effective against glucocorticoid-resistant T-ALL, identify glucocorticoids as critical regulators of cell fate determination and tissue homeostasis in the gut and suggest that cotreatment with glucocorticoids may facilitate the clinical development of GSIs by



protecting from the intestinal toxicity typically associated with inhibition of NOTCH signaling in the gut.

## Methods

### Inhibitors and drugs

Both compound E (CompE) [(2S)-2-[[[3,5-difluorophenyl)-acetylamino]-N-[(3S)-1-methyl-2-oxo-5-phenyl-2,3-dihydro-1H-1,4-benzodiazepin-3-yl] propanamide] (Alexis Biochemicals, Lausen, Switzerland) and DBZ (2S)-2-[2-(3,5-difluorophenyl)-acetylamino]-N-(5-methyl-6-oxo-6,7-dihydro-5H-dibenzo[b,d]azepin-7-yl)-propionamide (SYNCOM BV, Groningen, the Netherlands) are cell permeable, selective, nontransition state and noncompetitive inhibitors of the  $\gamma$ -secretase complex. Z-VAD, dexamethasone, etoposide, methotrexate, vincristine and RU486 were obtained from Sigma-Aldrich and L-asparaginase from Roche.

### Primary leukemia samples

Cryopreserved lymphoblast samples were provided by collaborating institutions in the US (Department of Pediatrics, Columbia Presbyterian Hospital, New York), the Netherlands (Erasmus MC-Sophia Children's Hospital, Rotterdam) and Italy (Hemato-Oncology Laboratory, Department of Pediatrics, University of Padua, Padua). All samples were collected with informed consent and under the supervision of local IRB committees.

### Cell viability studies, gene and protein expression analysis

Cell viability assays, retroviral and lentiviral transduction, microarray analysis, quantitative RT-PCR, luciferase reporter assays, chromatin immunoprecipitation, Western blot and immunohistochemistry assays were performed following standard procedures and are detailed in the supplementary methods online.

### Mice and animal procedures

All mice were kept in specific pathogen-free animal facilities at Memorial-Sloan Kettering Cancer Center, New York University Medical Center and Columbia University Medical Center. All animal procedures were performed in accord with the guidelines of the Institutional Animal Care and Use Committees at these institutions. Xenograft experiments were performed with 6 to 8-week-old NOD/SCID female mice (Taconic Farms) as recipients. Toxicity experiments were carried out in 6-week-old C57/Black6 female mice (Jackson Laboratory) and *Ccnd2* knockout mice. *Ccnd2* knockout mice have been described before 42. To analyze the effects of dexamethasone in GSI-induced toxicity we treated mice with vehicle (DMSO), dexamethasone (15 mg kg<sup>-1</sup>), DBZ (10  $\mu$ mol kg<sup>-1</sup>) and dexamethasone (15 mg kg<sup>-1</sup>) plus DBZ (10  $\mu$ mol kg<sup>-1</sup>) daily by intraperitoneal injection for 5 and 10 days. At the end of the treatment, animals were euthanized and tissues and organs were collected and processed for histological and immunohistochemical analysis.

Mice for inducible deletion of *CSL/RBPJ* were generated by breeding *RBPJ(f/f)* conditional knockout mice 47 to the *Cre-Tam* mouse line, which expresses a tamoxifen-inducible *Cre* from the ubiquitous *Rosa26* locus 37. *RBPJ(f/f) Cre-Tam* were treated with tamoxifen (1

mg) by oral gavage daily for 3 days to induce *RBPJ* deletion. To analyze the effect of dexamethasone treatment in the induction of goblet cell metaplasia induced by Notch inactivation via *RBPJ* deletion we injected *RBPJ(f/f) Cre-Tam* tamoxifen-treated mice with dexamethasone ( $15 \text{ mg kg}^{-1}$ ) (n=3) or vehicle only (n=3) via intraperitoneal injection for 10 days starting the first day of tamoxifen treatment. The effects of tamoxifen and dexamethasone treatment in the gut were evaluated via histological and immunohistochemical analysis.

Luminescent CUTLL1 cells were generated by infection of the CUTLL1 cell line with FUW-luc lentiviruses followed by selection with neomycin ( $1 \text{ mg ml}^{-1}$ ); luciferase expression was verified *in vitro* with the Dual-Luciferase Reporter Assay kit (Promega). For subcutaneous xenograft experiments, we injected  $2.5 \times 10^6$  T-ALL cells embedded in matrigel (BD Biosciences) in the flank. After 1 week, mice were segregated into treatment groups (6 animals per group) and treated daily with vehicle (DMSO), dexamethasone ( $15 \text{ mg kg}^{-1}$ ), DBZ ( $10 \text{ } \mu\text{mol kg}^{-1}$ ) or dexamethasone ( $15 \text{ mg kg}^{-1}$ ) plus DBZ ( $10 \text{ } \mu\text{mol kg}^{-1}$ ) by intraperitoneal injection. For imaging studies, mice were anesthetized by isoflurane inhalation and injected with D-luciferin at  $50 \text{ mg Kg}^{-1}$  (Xenogen) intraperitoneally. Photonic emission was imaged with the In Vivo Imaging System (IVIS, Xenogen) with a collection time of 1 minute. Tumor bioluminescence was quantified by integrating the photonic flux (photons per second) through a region encircling each tumor as determined by the LIVING IMAGES software package (Xenogen).

For intravenous xenograft transplantation, recipient animals were irradiated with a total X-ray dose of 300 cGy. Two million CUTLL1 cells expressing luciferase were injected via the tail vein. After a 3-week window for tumor engraftment, mice with homogeneous tumor burdens were segregated into treatment groups (8 animals per group) and treated daily with vehicle (DMSO), dexamethasone ( $15 \text{ mg kg}^{-1}$ ), DBZ ( $10 \text{ } \mu\text{mol kg}^{-1}$ ) or dexamethasone ( $15 \text{ mg kg}^{-1}$ ) plus DBZ ( $10 \text{ } \mu\text{mol kg}^{-1}$ ) by intraperitoneal injection for 14 days. Disease progression and therapy response were evaluated weekly using bioimaging as described above by integrating the photonic flux (photons per second) through a region around each mouse. Animals were followed up for up to 10 weeks. At the end of the observation period, single cell suspensions from the spleen of surviving animals were analyzed for the presence of leukemic cells by flow cytometry after staining with human anti CD45-FITC (BD Biosciences).

## Supplementary Material

Refer to Web version on PubMed Central for supplementary material.

## Acknowledgements

We thank U. Klein for help with flow cytometry analysis; T. Matos for the processing of histological, histochemical and immunohistochemical assays; P. Sicinski (Dana-Farber Cancer Institute) for the *Cend2* knockout mouse; T. Honjo (Kyoto University) and B. Reitzis (Columbia University) for the *RBPJ(f/f)* conditional knockout mouse, T. Ludwig for the *Cre-Tam* mouse line, A. Kung (Dana-Farber Cancer Institute) for the FUW-Luc neo vector; J. Aster (Brigham and Women's Hospital) for the MigR1 and MigR1-ICN1 retroviral constructs and for the NOTCH1-TAD antibody; W. Hahn (Dana-Farber Cancer Institute) for the pLKO shRNA vector, R. Dalla Favera (Columbia University) for the pCM8-cMYB vector, M. J. Garabedian (New York University) for the pCMV-HA-hGR vector and N. Wu and C. Wa for pharmacokinetic and drug metabolism analysis. This work was supported by

the National Institutes of Health (R01CA120196 and R01CA129382 to A.F. R56AI070310, 1R01CA105129 and 1R01CA133379 to I.A.); the WOLF Foundation (A.F.), the Leukemia and Lymphoma Society (grants 1287-08 and 6237-08 to A.F.), the Charlotte Geyer Foundation (A.F.), the Cancer Research Institute (A.F.), the Swim Across America Foundation (A.F.), the Golfers Against Cancer Foundation (A.F.), the American Cancer Society (RSG0806801 to I.A.) and the Fondo de Investigacion Sanitaria (grant CD07/00033 to P.J.R.). Adolfo Ferrando and Iannis Aifantis are Leukemia & Lymphoma Society Scholars. Teresa Palomero is a recipient of a Young Investigator Award from the Alex's Lemonade Stand Foundation. Irene Homminga is supported by the Dutch Cancer Society.

## References

1. Evin G, Sernee MF, Masters CL. Inhibition of gamma-secretase as a therapeutic intervention for Alzheimer's disease: prospects, limitations and strategies. *CNS Drugs*. 2006; 20:351–372. [PubMed: 16696577]
2. Selkoe D, Kopan R. Notch and Presenilin: regulated intramembrane proteolysis links development and degeneration. *Annu Rev Neurosci*. 2003; 26:565–597. [PubMed: 12730322]
3. Weng AP, et al. Activating mutations of NOTCH1 in human T cell acute lymphoblastic leukemia. *Science*. 2004; 306:269–271. [PubMed: 15472075]
4. Roy M, Pear WS, Aster JC. The multifaceted role of Notch in cancer. *Curr Opin Genet Dev*. 2007; 17:52–59. [PubMed: 17178457]
5. Deangelo D, et al. A phase I clinical trial of the notch inhibitor MK-0752 in patients with T-cell acute lymphoblastic leukemia/lymphoma (T-ALL) and other leukemias. *Journal of Clinical Oncology*, 2006 ASCO Annual Meeting Proceedings Part I. 2006; 24:6585.
6. Palomero T, et al. CUTLL1, a novel human T-cell lymphoma cell line with t(7;9) rearrangement, aberrant NOTCH1 activation and high sensitivity to gamma-secretase inhibitors. *Leukemia*. 2006; 20:1279–1287. [PubMed: 16688224]
7. Lewis HD, et al. Apoptosis in T cell acute lymphoblastic leukemia cells after cell cycle arrest induced by pharmacological inhibition of notch signaling. *Chem Biol*. 2007; 14:209–219. [PubMed: 17317574]
8. Milano J, et al. Modulation of notch processing by gamma-secretase inhibitors causes intestinal goblet cell metaplasia and induction of genes known to specify gut secretory lineage differentiation. *Toxicol Sci*. 2004; 82:341–358. [PubMed: 15319485]
9. van Es JH, et al. Notch/gamma-secretase inhibition turns proliferative cells in intestinal crypts and adenomas into goblet cells. *Nature*. 2005; 435:959–963. [PubMed: 15959515]
10. Wong GT, et al. Chronic treatment with the gamma-secretase inhibitor LY-411,575 inhibits beta-amyloid peptide production and alters lymphopoiesis and intestinal cell differentiation. *J Biol Chem*. 2004; 279:12876–12882. [PubMed: 14709552]
11. Searfoss GH, et al. Adipsin, a biomarker of gastrointestinal toxicity mediated by a functional gamma-secretase inhibitor. *J Biol Chem*. 2003; 278:46107–46116. [PubMed: 12949072]
12. Pear WS, Radtke F. Notch signaling in lymphopoiesis. *Semin Immunol*. 2003; 15:69–79. [PubMed: 12681943]
13. Ciofani M, Zuniga-Pflucker JC. Notch promotes survival of pre-T cells at the beta-selection checkpoint by regulating cellular metabolism. *Nat Immunol*. 2005; 6:881–888. [PubMed: 16056227]
14. Deftos ML, He YW, Ojala EW, Bevan MJ. Correlating notch signaling with thymocyte maturation. *Immunity*. 1998; 9:777–786. [PubMed: 9881968]
15. Aster JC, Pear WS, Blacklow SC. Notch Signaling in Leukemia. *Annu Rev Pathol*. 2008; 3:587–613. [PubMed: 18039126]
16. Palomero T, Dominguez M, Ferrando AA. The role of the PTEN/AKT Pathway in NOTCH1-induced leukemia. *Cell Cycle*. 2008; 7:965–970. [PubMed: 18414037]
17. Palomero T, Ferrando A. Oncogenic NOTCH1 control of MYC and PI3K: challenges and opportunities for anti-NOTCH1 therapy in T-cell acute lymphoblastic leukemias and lymphomas. *Clin Cancer Res*. 2008; 14:5314–5317. [PubMed: 18765521]
18. Seiffert D, et al. Presenilin-1 and -2 are molecular targets for gamma-secretase inhibitors. *J Biol Chem*. 2000; 275:34086–34091. [PubMed: 10915801]

19. Palomero T, et al. NOTCH1 directly regulates c-MYC and activates a feed-forward-loop transcriptional network promoting leukemic cell growth. *Proc Natl Acad Sci U S A*. 2006; 103:18261–18266. [PubMed: 17114293]
20. Palomero T, et al. Mutational loss of PTEN induces resistance to NOTCH1 inhibition in T-cell leukemia. *Nat Med*. 2007; 13:1203–1210. [PubMed: 17873882]
21. Eisen LP, Elsasser MS, Harmon JM. Positive regulation of the glucocorticoid receptor in human T-cells sensitive to the cytolytic effects of glucocorticoids. *J Biol Chem*. 1988; 263:12044–12048. [PubMed: 3261297]
22. Ramdas J, Liu W, Harmon JM. Glucocorticoid-induced cell death requires autoinduction of glucocorticoid receptor expression in human leukemic T cells. *Cancer Res*. 1999; 59:1378–1385. [PubMed: 10096574]
23. Levine EG, Peterson BA, Smith KA, Hurd DD, Bloomfield CD. Glucocorticoid receptors in chronic lymphocytic leukemia. *Leuk Res*. 1985; 9:993–999. [PubMed: 4046634]
24. Leventhal BG. Glucocorticoid receptors in lymphoid tumors. *Cancer Res*. 1981; 41:4861–4862. [PubMed: 6975165]
25. Pedersen KB, Vedeckis WV. Quantification and glucocorticoid regulation of glucocorticoid receptor transcripts in two human leukemic cell lines. *Biochemistry*. 2003; 42:10978–10990. [PubMed: 12974633]
26. Pedersen KB, Geng CD, Vedeckis WV. Three mechanisms are involved in glucocorticoid receptor autoregulation in a human T-lymphoblast cell line. *Biochemistry*. 2004; 43:10851–10858. [PubMed: 15323545]
27. Renner K, Ausserlechner MJ, Kofler RA. conceptual view on glucocorticoid-induced apoptosis, cell cycle arrest and glucocorticoid resistance in lymphoblastic leukemia. *Curr Mol Med*. 2003; 3:707–717. [PubMed: 14682492]
28. Geley S, et al. Resistance to glucocorticoid-induced apoptosis in human T-cell acute lymphoblastic leukemia CEM-C1 cells is due to insufficient glucocorticoid receptor expression. *Cancer Res*. 1996; 56:5033–5038. [PubMed: 8895760]
29. Schmidt S, et al. Glucocorticoid resistance in two key models of acute lymphoblastic leukemia occurs at the level of the glucocorticoid receptor. *Faseb J*. 2006; 20:2600–2602. [PubMed: 17077285]
30. Breslin MB, Geng CD, Vedeckis WV. Multiple promoters exist in the human GR gene, one of which is activated by glucocorticoids. *Mol Endocrinol*. 2001; 15:1381–1395. [PubMed: 11463861]
31. Geng CD, Vedeckis WV. c-Myb and members of the c-Ets family of transcription factors act as molecular switches to mediate opposite steroid regulation of the human glucocorticoid receptor 1A promoter. *J Biol Chem*. 2005; 280:43264–43271. [PubMed: 16263717]
32. Nunez BS, Vedeckis WV. Characterization of promoter 1B in the human glucocorticoid receptor gene. *Mol Cell Endocrinol*. 2002; 189:191–199. [PubMed: 12039077]
33. Erlacher M, et al. BH3-only proteins Puma and Bim are rate-limiting for gamma-radiation- and glucocorticoid-induced apoptosis of lymphoid cells in vivo. *Blood*. 2005; 106:4131–4138. [PubMed: 16118324]
34. Abrams MT, Robertson NM, Yoon K, Wickstrom E. Inhibition of glucocorticoid-induced apoptosis by targeting the major splice variants of BIM mRNA with small interfering RNA and short hairpin RNA. *J Biol Chem*. 2004; 279:55809–55817. [PubMed: 15509554]
35. Wang Z, Malone MH, He H, McColl KS, Distelhorst CW. Microarray analysis uncovers the induction of the proapoptotic BH3-only protein Bim in multiple models of glucocorticoid-induced apoptosis. *J Biol Chem*. 2003; 278:23861–23867. [PubMed: 12676946]
36. Puthalakath H, et al. Bmf: a proapoptotic BH3-only protein regulated by interaction with the myosin V actin motor complex, activated by anoikis. *Science*. 2001; 293:1829–1832. [PubMed: 11546872]
37. Guo K, et al. Disruption of peripheral leptin signaling in mice results in hyperleptinemia without associated metabolic abnormalities. *Endocrinology*. 2007
38. Katz JP, et al. The zinc-finger transcription factor Klf4 is required for terminal differentiation of goblet cells in the colon. *Development*. 2002; 129:2619–2628. [PubMed: 12015290]

39. Wei D, Kanai M, Huang S, Xie K. Emerging role of KLF4 in human gastrointestinal cancer. *Carcinogenesis*. 2006; 27:23–31. [PubMed: 16219632]
40. Jensen J, et al. Control of endodermal endocrine development by Hes-1. *Nat Genet*. 2000; 24:36–44. [PubMed: 10615124]
41. Stappenbeck TS, Wong MH, Saam JR, Mysorekar IU, Gordon JI. Notes from some crypt watchers: regulation of renewal in the mouse intestinal epithelium. *Curr Opin Cell Biol*. 1998; 10:702–709. [PubMed: 9914172]
42. Sicinski P, et al. Cyclin D2 is an FSH-responsive gene involved in gonadal cell proliferation and oncogenesis. *Nature*. 1996; 384:470–474. [PubMed: 8945475]
43. Wei G, et al. Gene expression-based chemical genomics identifies rapamycin as a modulator of MCL1 and glucocorticoid resistance. *Cancer Cell*. 2006; 10:331–342. [PubMed: 17010674]
44. Jang J, et al. Notch1 confers thymocytes a resistance to GC-induced apoptosis through Deltex1 by blocking the recruitment of p300 to the SRG3 promoter. *Cell Death Differ*. 2006; 13:1495–1505. [PubMed: 16341126]
45. Choi YI, et al. Notch1 confers a resistance to glucocorticoid-induced apoptosis on developing thymocytes by down-regulating SRG3 expression. *Proc Natl Acad Sci U S A*. 2001; 98:10267–10272. [PubMed: 11504912]
46. Jeon SH, et al. A new mouse gene, SRG3, related to the SWI3 of *Saccharomyces cerevisiae*, is required for apoptosis induced by glucocorticoids in a thymoma cell line. *J Exp Med*. 1997; 185:1827–1836. [PubMed: 9151708]
47. Han H, et al. Inducible gene knockout of transcription factor recombination signal binding protein-J reveals its essential role in T versus B lineage decision. *Int Immunol*. 2002; 14:637–645. [PubMed: 12039915]

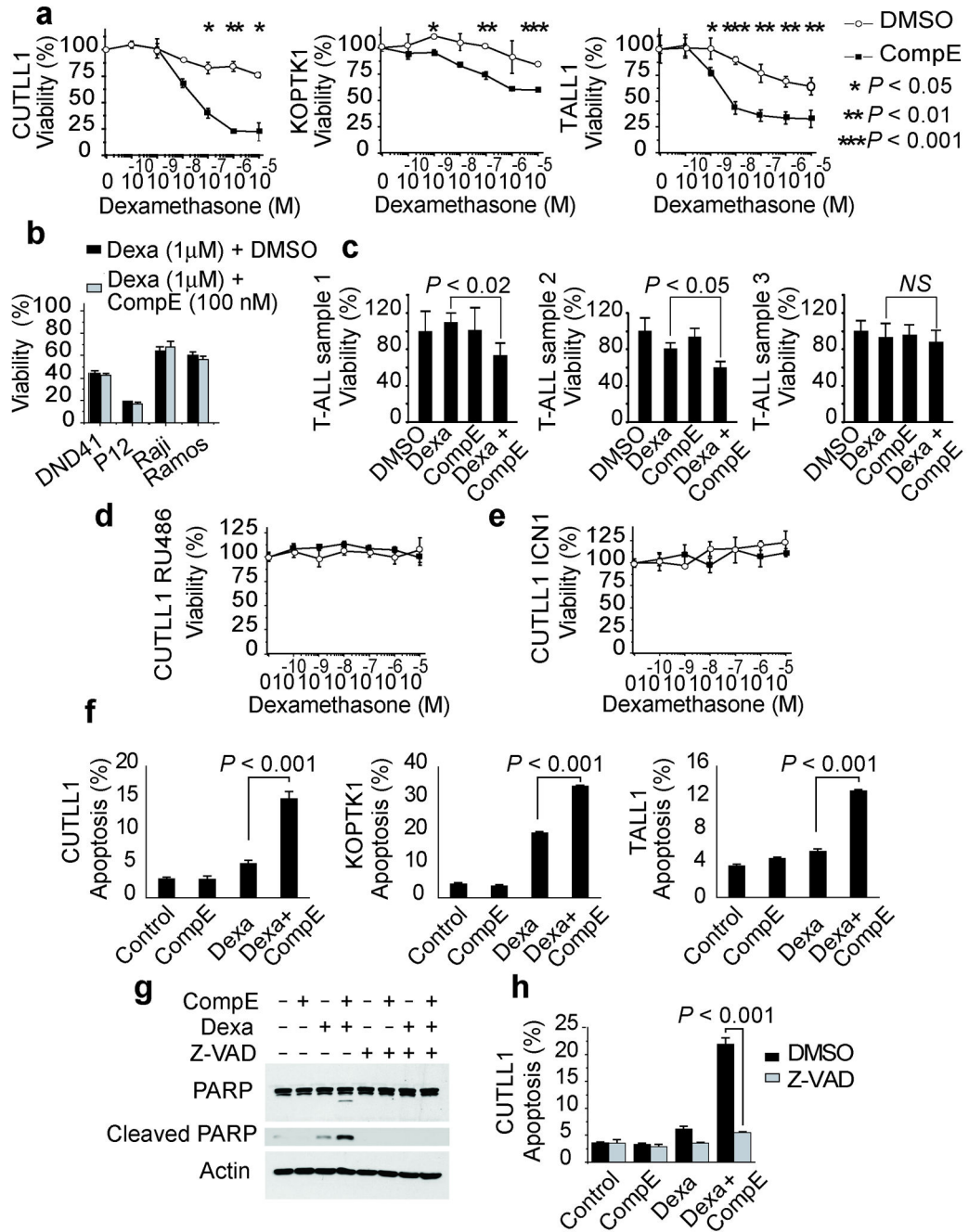


**Figure 1.**

GSI reverse glucocorticoid resistance in T-ALL cells. (a) Viability assays in the glucocorticoid-resistant T-ALL cell lines CUTLL1 (72 h), KOPTK1 (48 h) and TALL1 (72 h) treated with 100nM CompE (black squares) or vehicle only (open circles) plus increasing concentrations of dexamethasone. (b) Analysis of T-ALL cell lines sensitive to glucocorticoids (DND41, P12 ICHIKAWA) or B-lineage cell lines (Raji and Ramos). (c) Analysis of in primary T-ALL samples resistant to glucocorticoids. (d) Analysis of CUTLL1 cells treated with glucocorticoid receptor antagonist RU486 (1  $\mu$ M). (e) Analysis of



CUTLL1 cells expressing constitutively active intracellular NOTCH1 (ICN1). **(f)** Percentage of apoptotic cells (annexinV positive/PI negative) in CUTLL1 (72 h), KOPTK1 (48 h) and TALL1 cells (72 h) treated with DMSO (control), CompE (100 nM), dexamethasone (1  $\mu$ M) and dexamethasone (1  $\mu$ M) plus CompE (100 nM). **(g,h)** Inhibition of apoptosis induction by dexamethasone plus CompE cotreatment by the Z-VAD caspase inhibitor as demonstrated by inhibition of PARP cleavage by Western blot **(g)** and decreased annexinV positive/PI negative cells by flow cytometry **(h)**. Data in a-f and h are means  $\pm$  SD of triplicate experiments. Statistical significance was assessed with Student's *t*-test.

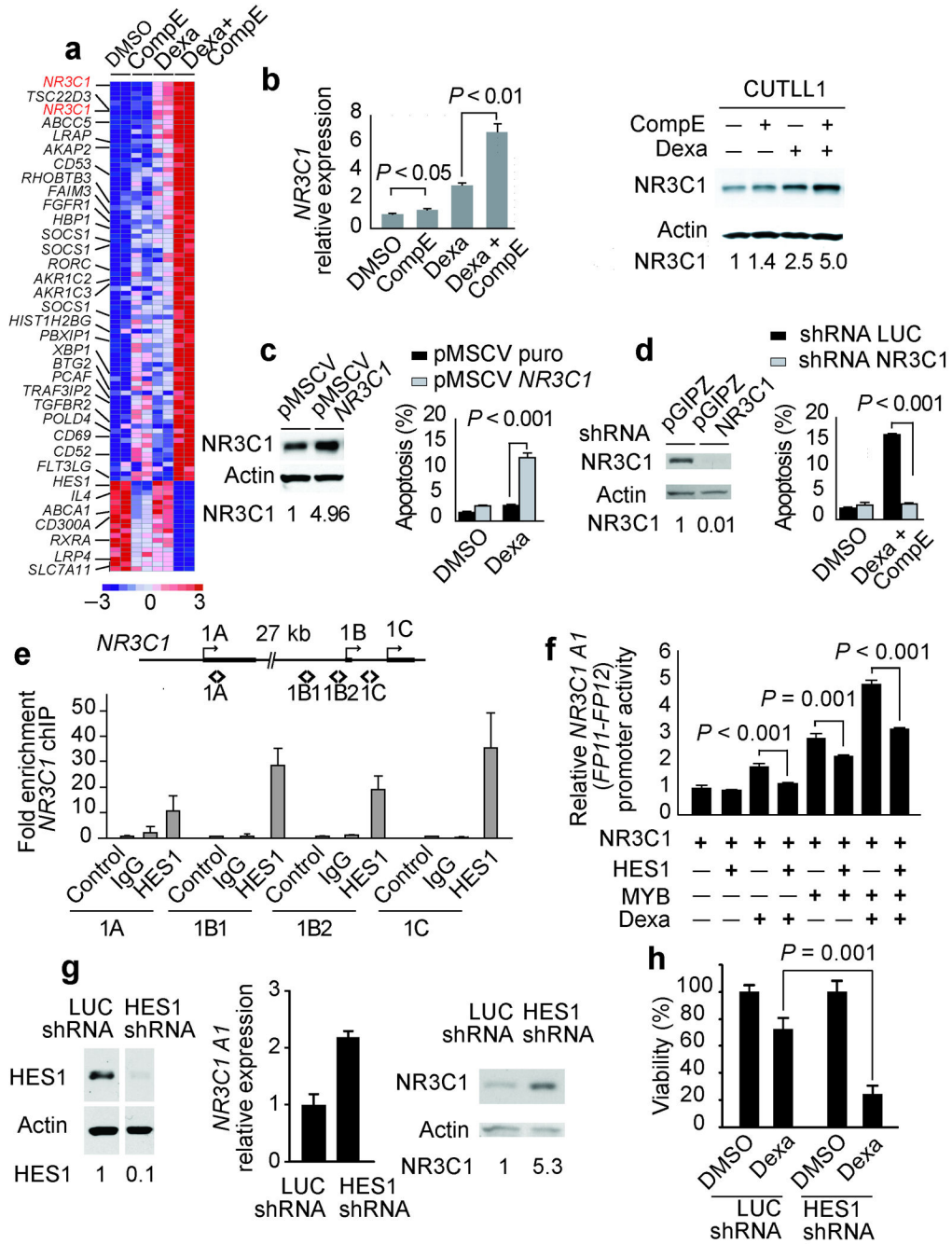


**Figure 2.** Inhibition of NOTCH1-HES1 signaling restores glucocorticoid receptor autoregulation. (a) Microarray gene expression changes in CUTLL1 cells at 24 h treated with DMSO, CompE, dexamethasone and CompE plus dexamethasone. Relative expression levels are color coded as indicated at the bottom. (b) Quantitative RT-PCR analysis of the glucocorticoid receptor gene (*NR3C1*) and Western blot analysis and quantitation of glucocorticoid receptor protein levels in CUTLL1 cells treated with dexamethasone and CompE compared with vehicle only (DMSO). (c) Western blot analysis of NR3C1 levels and induction of apoptosis by

dexamethasone and CompE in CUTLL1 cells infected with retroviruses expressing the glucocorticoid receptor (pMSCV *NR3C1*). **(d)** Analysis of apoptosis induction by dexamethasone plus CompE in CUTLL1 cells infected with shRNA lentiviruses targeting the glucocorticoid receptor (pGIPZ *NR3C1*) **(e)** Quantitative ChIP analysis of HES1 binding to *NR3C1* promoter sequences. **(f)** Effects of *HES1*, *MYB* and dexamethasone (1  $\mu$ M) in the activity of a human *NR3C1 A1* reporter. Luciferase activity is shown relative to an internal control expressing *Renilla* luciferase. **(g,h)** *NR3C1* expression **(g)** and analysis of apoptosis **(h)** in CUTLL1 cells treated with dexamethasone and CompE after lentiviral shRNA knockdown of HES1 (HES1 shRNA). A shRNA targeting the luciferase gene (shRNA LUC) was used as control. Drug concentrations in **a–c** were CompE 100 nM and dexamethasone 1  $\mu$ M. Bars represent means  $\pm$  SD of triplicate experiments. Statistical significance was assessed with Student's *t*-test. HES1 and *NR3C1* relative protein levels are indicated at the bottom of corresponding lanes in the Western blot.

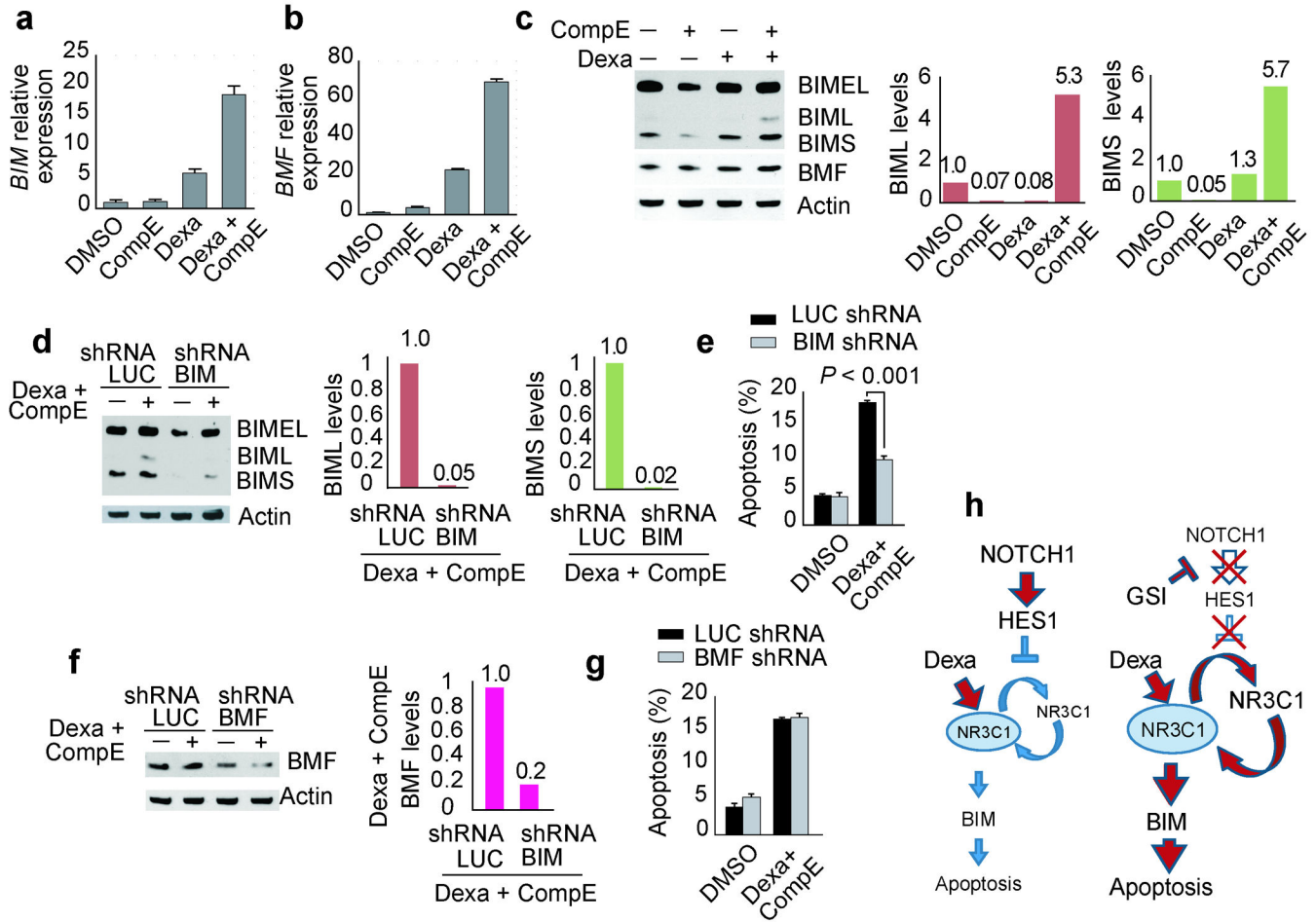


**Figure 3.** *BIM* upregulation reverses glucocorticoid resistance in T-ALL cells treated with dexamethasone plus CompE. **(a, b)** Quantitative RT-PCR analysis of the BH3-only factors *BIM* **(a)** and *BMF* **(b)** in CUTLL1 cells treated with dexamethasone and/or CompE compared with vehicle only (DMSO). Relative expression levels are shown normalized to those of vehicle-only controls. **(c)** Western blot analysis and quantitation of BIM and BMF in CUTLL1 cells treated with dexamethasone and/or CompE compared with vehicle only (DMSO). **(d)** Western blot analysis of BIM following sRNA knock down. CUTLL1 cells infected with control lentivirus targeting the luciferase gene (pLKO LUC) or *BIM* (pLKO BIM) were treated with vehicle only or dexamethasone plus CompE for 24 hours and analyzed by Western blotting. **(e)** Induction of apoptosis in control (pLKO LUC infected) and BIM knockdown (pLKO BIM infected) cells treated with dexamethasone plus CompE. **(f)** Western blot analysis of BMF by shRNA knock down. CUTLL1 cells infected with control lentivirus targeting the luciferase gene (pLKO LUC) or *BMF* (pLKO BMF) were treated with vehicle only or dexamethasone plus CompE for 24 hours and analyzed by Western blot. **(g)** Induction of apoptosis in control (pLKO LUC infected) and BMF knockdown (pLKO BMF-infected) cells treated with dexamethasone plus CompE. Apoptosis refers to the percentage of annexin V positive/PI negative cells. **(h)** Schematic

representation of the transcriptional regulatory network controlling glucocorticoid receptor autoregulation downstream of NOTCH1 and dexamethasone-induced apoptosis upon inhibition of NOTCH1 signaling via GSI treatment.

Author Manuscript

Author Manuscript

Author Manuscript

Author Manuscript

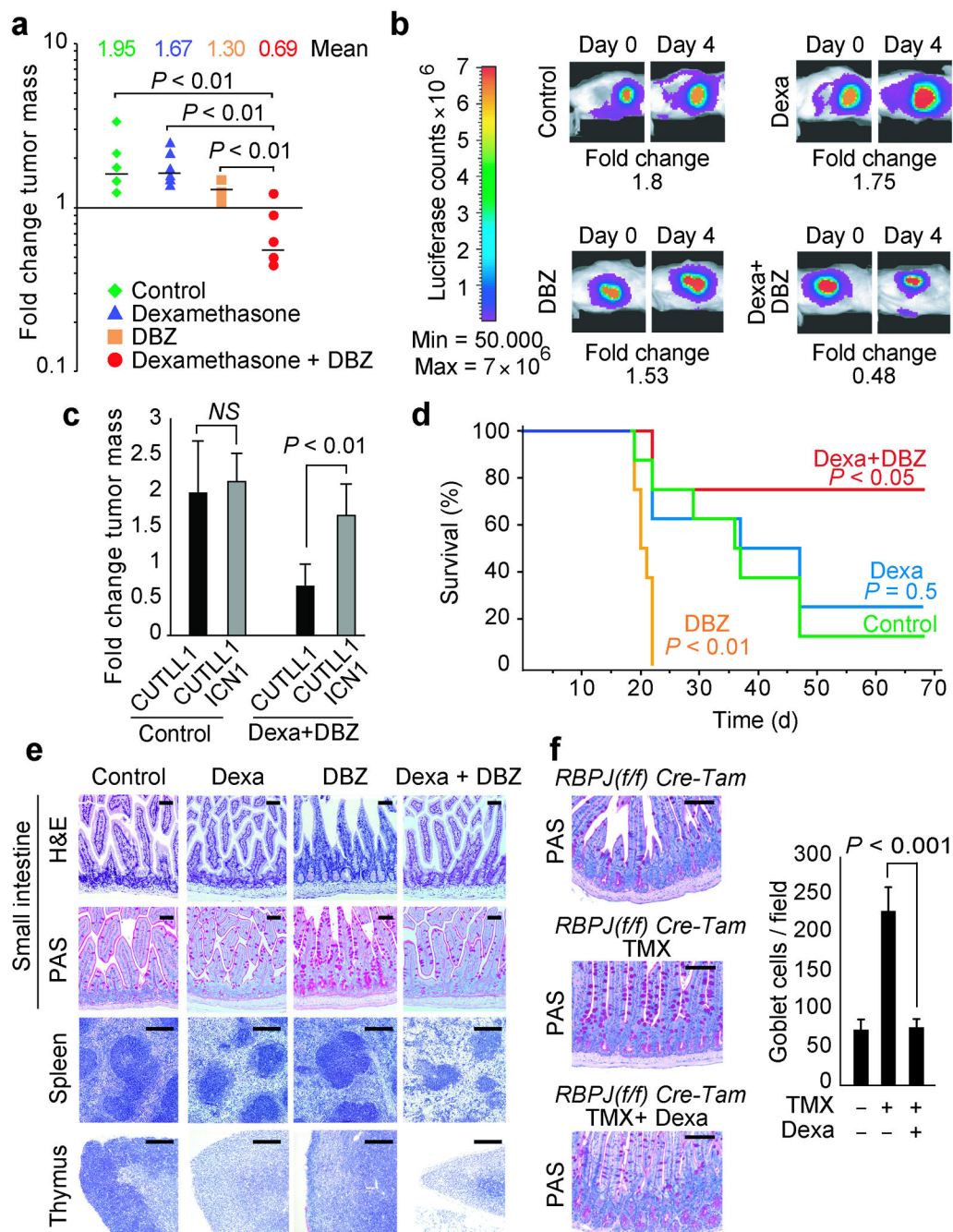


**Figure 4.** Interaction of NOTCH inhibition and dexamethasone treatment in tumor response and gut toxicity *in vivo*. **(a)** Bioimaging quantitation of tumor mass changes in subcutaneous CUTLL1 T-ALL xenografts in mice treated with vehicle (control), dexamethasone, GSI (DBZ) or GSI plus dexamethasone (Dexamethasone + DBZ) for 4 days. **(b)** Representative examples of bioluminescence *in vivo* imaging showing changes in tumor load in representative mice (animals with closest values to the median are shown) treated with vehicle (control), dexamethasone (Dexa), DBZ and dexamethasone plus DBZ (Dexa +



DBZ). (c) Tumor mass changes induced by dexamethasone plus DBZ treatment compared to controls in CUTLL1 T-ALL xenografts (CUTLL1) and CUTLL1 xenografts expressing an intracellular form of NOTCH1 (CUTLL1 ICN1), which does not require  $\gamma$ -secretase cleavage for activation. (d) Kaplan-Meier plot of overall survival among mice treated with vehicle (Control), dexamethasone, DBZ or DBZ plus dexamethasone after xenograft transplantation of human T-ALL cells via tail vein injection. (e) Histological analysis of small intestine, spleen and thymus from mice treated with vehicle, dexamethasone, DBZ and dexamethasone plus DBZ for 5 days. (f) Goblet cell analysis and quantitation in the ileum of *RBPJ(fl/fl) Cre-Tam* conditional knockout mice in basal conditions (*RBPJ(fl/fl) Cre-Tam*), following conditional deletion of *CSL/RBPJ* with tamoxifen (*RBPJ(fl/fl) Cre-Tam* TMX) and upon conditional deletion of *CSL/RBPJ* followed by dexamethasone treatment (*RBPJ(fl/fl) Cre-Tam* TMX + Dexa). TMX: tamoxifen. H&E: haemotoxylin and eosin staining. Scale bars represent 100  $\mu$ m in the intestine and 400  $\mu$ m in spleen and thymus.

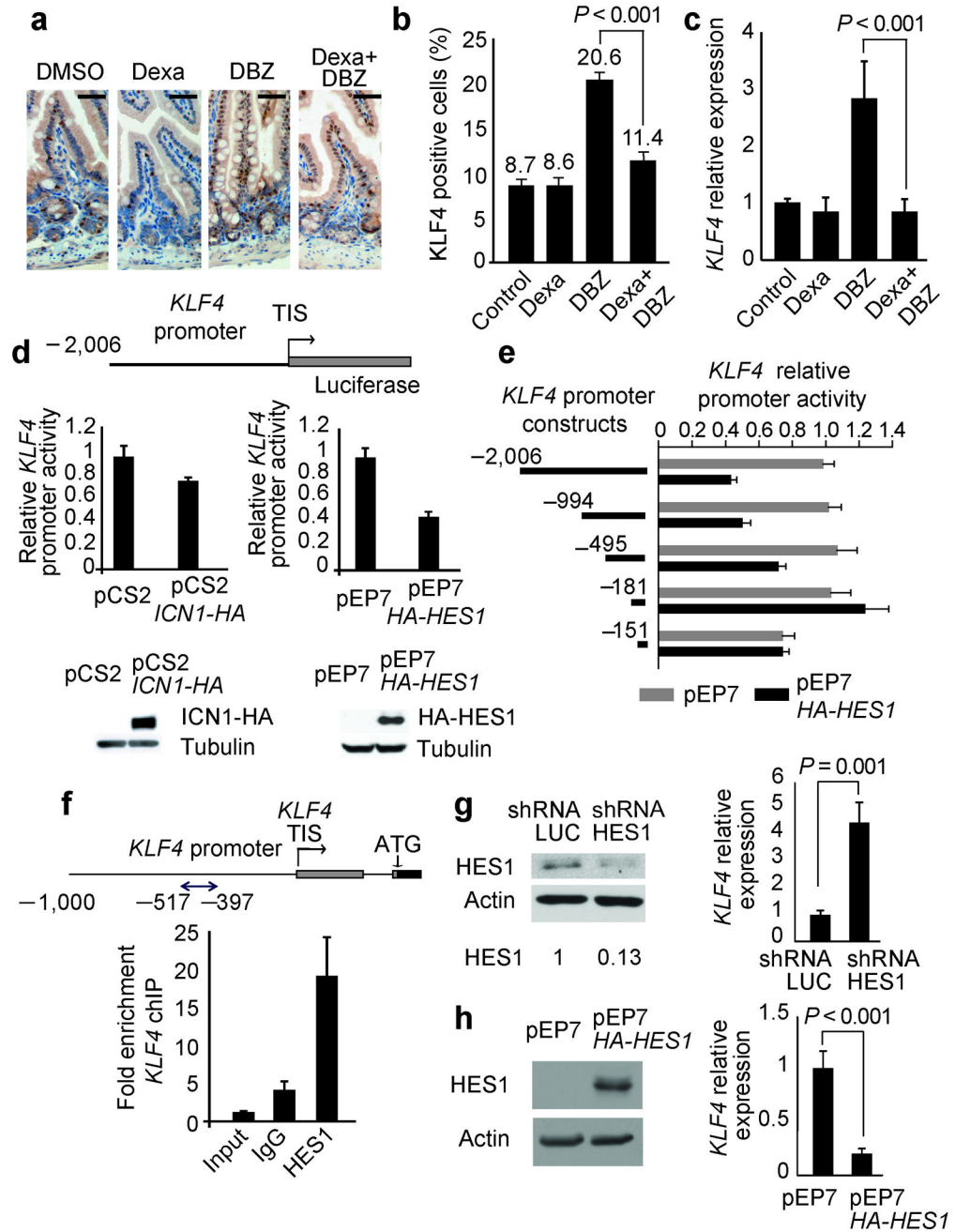


**Figure 5.** NOTCH-HES1 signaling regulates *KLF4* expression in the gut. **(a,b)** Immunohistochemistry analysis of *Klf4* expression in small intestine of mice treated with dexamethasone, DBZ or the combination of dexamethasone plus DBZ for 5 days. Scale bars represent 100  $\mu$ m. **(c)** Real-time PCR analysis of *Klf4* transcript levels in small intestine of mice treated with dexamethasone, DBZ or the combination of dexamethasone plus DBZ for 10 days. *Gapdh* levels were used as a reference control. Data are means  $\pm$  SD of three animals per group. **(d–e)** Effects of *ICN1* and *HES1* expression in human *KLF4* promoter activity. Luciferase

reporter assays were performed in AGS cells with reporter constructs encompassing 2,006 bp (**d**, **e**), 994, 495 and 181 nucleotides (**e**) of the *KLF4* promoter. Promoter activity is shown relative to an internal control expressing *Renilla* luciferase. Western blot shows expression of ICN1-HA and HA-HES1 proteins in AGS cells transfected with *ICN1* and *HES1* expression plasmids. (**f**) Quantitative ChIP analysis of HES1 binding to *KLF4* promoter sequences. (**g**) Lentiviral shRNA knockdown of *HES1* in AGS cells induces transcriptional upregulation of *KLF4*. (**h**) Expression of HA-HES1 protein in AGS cells induces transcriptional downregulation of *KLF4*. Expression of a control shRNA targeting the luciferase gene (shRNA LUC) was used as control. Bars represent means  $\pm$  SD of triplicate experiments. TIS: transcription initiation site. HES1 protein levels normalized to the loading control are shown at the bottom of corresponding lanes in the Western blot.

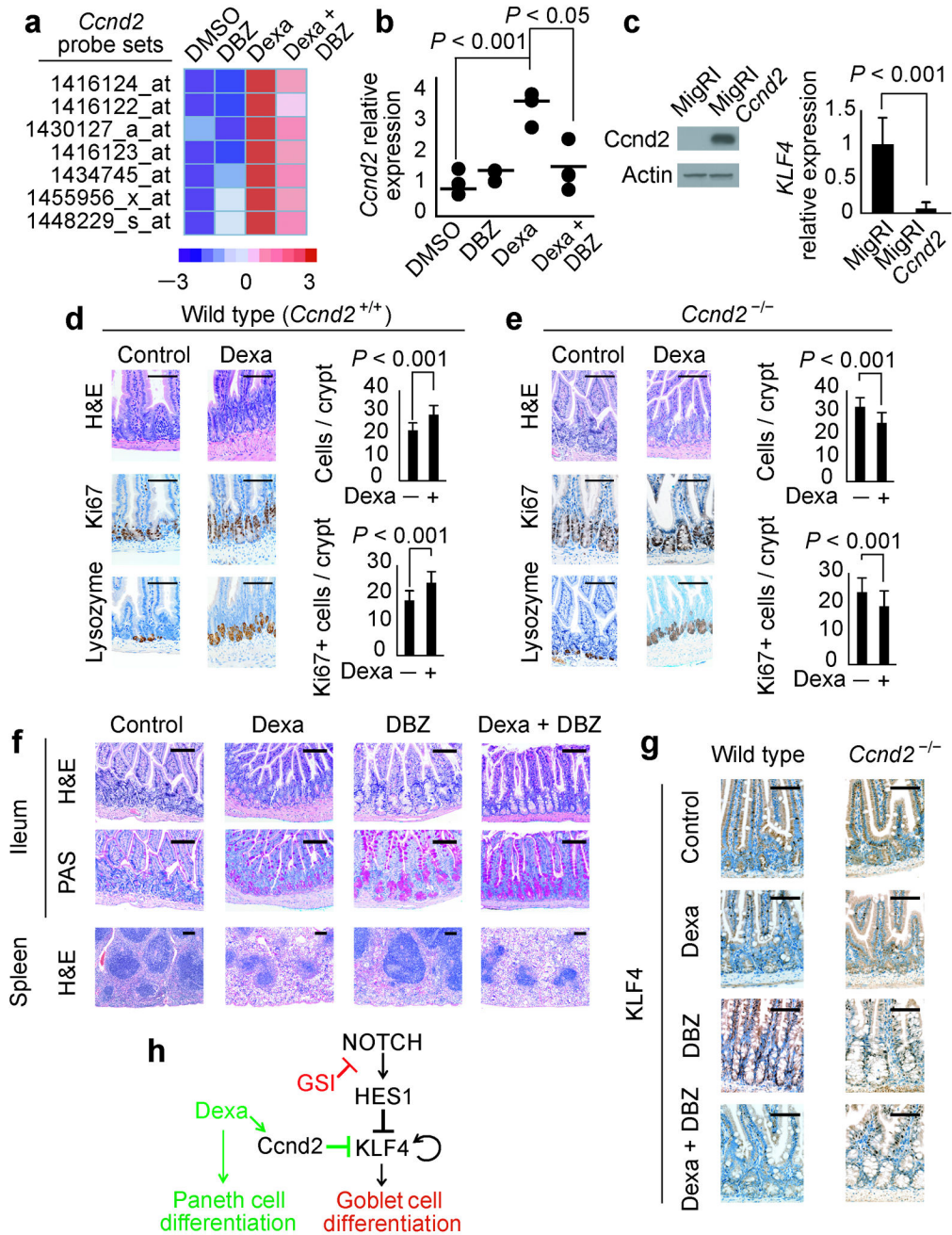


**Figure 6.** Glucocorticoid-induced *Ccnd2* upregulation mediates the enteroprotective effect of dexamethasone against GSI-induced gut toxicity. (a) Microarray analysis of *Ccnd2* transcript levels in the small intestine of mice treated with vehicle (DMSO), DBZ, dexamethasone (Dexa) and dexamethasone plus DBZ (Dexa + DBZ) for 5 days. The heat map diagram shows average values from duplicate samples. (b) Quantitative RT-PCR analysis of the *Ccnd2* gene in the small intestine of mice treated with vehicle (DMSO), DBZ, dexamethasone (Dexa) and dexamethasone plus DBZ (Dexa + DBZ). Horizontal bars

indicate the mean expression level in each group. **(c)** Retroviral expression of *Ccnd2* in AGS cells induces transcriptional downregulation of *KLF4*. **(d, e)** Histological and histochemical analysis of small intestines from wild type **(d)** and *Ccnd2*<sup>-/-</sup> mice **(e)** treated with vehicle only (Control) or dexamethasone (Dexa). **(f)** Histological and histochemical studies of small intestines and spleens from *Ccnd2*<sup>-/-</sup> mice treated with vehicle only (DMSO), dexamethasone, DBZ and dexamethasone plus DBZ for 10 days. H&E: haemotoxylin and eosin staining. Scale bars represent 100 µm. **(g)** Immunohistochemistry analysis of Klf4 expression in small intestine of wild type and *Ccnd2*<sup>-/-</sup> mice treated with dexamethasone, DBZ or the combination of dexamethasone plus DBZ for 5 days. Scale bars represent 100 µm. **(h)** Schematic representation of the transcriptional regulatory network controlling cell differentiation in the intestinal cells downstream of Notch and glucocorticoid receptor signaling.